Structure, Morphology, and Properties of Methyl-Pendant Poly(*p*-phenylene benzobisimidazole) and Methyl-Pendant Poly(*p*-phenylene benzobisthiazole)

Shawn Jenkins,[†] Karl I. Jacob,[†] Malcolm B. Polk,[†] Satish Kumar,*[,†] T. D. Dang,[‡] and F. E. Arnold[‡]

School of Textile and Fiber Engineering, Georgia Institute of Technology, Atlanta Georgia, 30332-0295, and AFRL, Wright Patterson Air Force Base, Dayton, OH, 45433

Received May 8, 2000; Revised Manuscript Received July 31, 2000

ABSTRACT: Monomethyl-pendant poly(*p*-phenylene benzobisimidazole) (MePBI) has been spun into fiber and compared with an analogous methyl-pendant poly(*p*-phenylene benzobisthiazole) (MePBZT). From FTIR and WAXD, the former system has been found to exhibit intermolecular hydrogen bonding, while the latter possesses only weak van der Waals interactions. The thermomechanical properties of both systems, as examined by TGA, TMA, and DMS, are presented and discussed. A crystal structure of MePBI is proposed, which suggests intermolecular hydrogen bonding only between pairs of chains within the MePBI crystal. As compared to MePBZT and other rigid-rod polymers where the intermolecular hydrogen bond is not present, MePBI has higher compressive strength. The relatively high compressive strength of MePBI is attributed to increased intermolecular association, as opposed to differences in morphology.

Introduction

For some time, it has been of interest to develop rigid-rod polymers having the capacity to form intermolecular hydrogen bonds, the primary motivation for such work being to improve fiber axial compressive strength. Somewhat higher compressive strength of poly(*p*-phenylene terephthalamide) (PPTA) over that of other polymeric fibers is thought to be a consequence of hydrogen bonding.[1] Interest in such materials has led to the development of the rigid-rod polymer, poly(diimadazopyridinylene dihydroxy-phenylene) (PIPD), by Akzo Nobel.[2] The crystal structure of PIPD has been reported to contain bidirectional hydrogen bonding,[3] with the intermolecular hydrogen-bonding energy per chain being on the order of 22.6 kcal/mol.[4] The relatively high compressive strength of PIPD has been attributed to the presence of this hydrogen-bonded network. [5]

One of the first of several rigid-rod systems to be developed was poly(*p*-phenylene benzobisimidazole) (PBI). However, detailed work on this structure was not reported, as only limited molecular weight polymer could be produced, as PBI crystallized out of solution during polymerization.[6] Attempts to introduce hydrogen-bonding capability into the structure of poly(*p*-phenylene benzobisthiazole) (PBZT) were made by incorporating pendant hydroxy groups on the phenyl ring.[7] The compressive strength of dihydroxy-PBZT was found to decrease relative to that of unmodified PBZT. The lack of improvement in compressive strength was attributed to the formation of *intra*molecular, rather than *inter*-molecular, hydrogen bonds.[7] A review of rigid-rod polymers with enhanced lateral interactions has recently been published.[8]

The tendency for PBI to prematurely crystallize out of solution during synthesis was diminished by incorporating a methyl-pendant group on the phenyl ring.[9] However, neither mechanical properties nor structural information, pertaining to monomethyl-pendant PBI, was reported upon achieving higher molecular weight. The placement of two methyl groups on the phenyl ring of PBI, through the use of 2,5-dimethylterephthalic acid, was found to again result in premature crystallization out of solution.[10] Presumably, this was due to symmetry introduced into the system by the presence of two methyl groups. In this paper, the structure, morphology, and properties of monomethyl-pendant PBI (MePBI) fiber have been investigated. For comparison, work done on monomethyl-pendant PBZT (MePBZT), which does not exhibit hydrogen bonding, is also reported. Chemical structures of these systems are given in Figure 1.

Experimental Section

Fiber Spinning and Heat Treatment. The synthesis of MePBI has been reported previously.[9] Ten weight percent polymer in polyphosphoric acid was used for fiber spinning. The intrinsic viscosity of MePBI and MePBZT was 11 and 15 dL/g, respectively. The polymers were dry-jet wet spun using a 250-mm diameter single-hole spinneret and an air gap of ≈15 cm. Spinning temperatures of 110 and 90 °C were used for MePBI and MePBZT, respectively. Prior to spinning, the solutions were preheated for ≈4 h at the spinning temperature. Upon spinning, the fibers were coagulated in distilled water at room temperature and then vacuum-dried at 100 °C overnight. Spin draw ratios as high as 20 were possible in the spinning of MePBI, compared to 12 in the case of MePBZT.

Cleaving of the pendant group in MePBZT is known to occur around 425 °C.[9] Thus, after spinning, fibers were heat-treated at 390 °C under tension (unless otherwise noted), in an attempt to improve crystalline order within the fiber without inducing chemical reactions. Heat treatment was carried out in a tube furnace under nitrogen.

Material Characterization. Thermogravimetric analysis was carried out on a Seiko 320 TG/DTA at 10 °C/min under N_2. Thermomechanical analysis was performed, under N_2, using a TMA from TA Instruments. A stress level of ≈50 MPa was used to keep the fiber taut during TMA testing. Dynamic mechanical properties were evaluated using a Seiko 210 DMS. Fibers 20 mm in length were subjected to a displacement amplitude of 10 mm and a frequency of 1 Hz. The DMS tests were conducted at a heating rate of 3 °C/min in air. Variable temperature FTIR was performed on films in nitrogen using a Brüker Vector 22 IR with a Harrick high-temperature cell. Films were made by dissolving fiber in methane sulfonic acid.

* To whom correspondence should be addressed.
[†] Georgia Institute of Technology.
[‡] Wright Patterson Air Force Base.

10.1021/ma000790x CCC: $19.00
Published on Web 10/25/2000

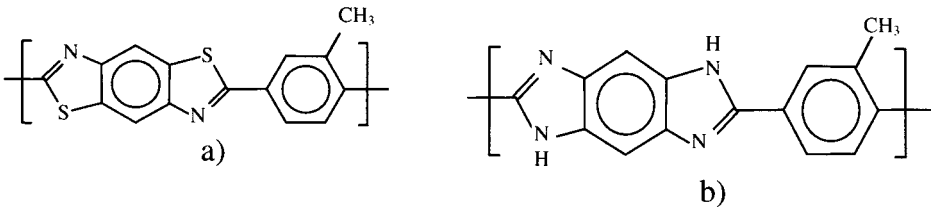

Figure 1. Chemical structures of (a) methyl-pendant poly(*p*-phenylene benzobisthiazole) (MePBZT) and (b) methyl-pendant poly(*p*-phenylene benzobisimidazole) (MePBI).

The solution was cast in a glass dish and coagulated in distilled water for ≈1 week. Coagulated film was vacuum-dried at 100 °C overnight. The film morphology and structure, particularly orientation, is expected to be much different than that of the fiber. Scanning electron microscopy was carried out using a Hitachi S-800 microscope with a field emission electron gun (LaB_6). Samples were attached to aluminum stubs, using carbon tabs, and sputter-coated with gold (≈20-nm thick).

A Rigaku Rotaflex rotating anode diffractometer was used to obtain WAXD scans in the transmission mode using pinhole collimation. Cu Kα radiation was used in all experiments, with the X-ray generator being operated at 45 kV and 100 mA. The Kβ component of the incident beam was minimized using a nickel filter.

A model for the crystal structure of MePBI was built and the WAXD pattern simulated using the Cerius2 v. 2.0 software from Molecular Simulations Inc. Energy minimization of the unit cell was done using the COMPASS force field. In the process, WAXD-derived cell parameters were held constant. Unconstrained minimization using the COMPASS, UNIVERSAL, and CVFF force fields did not satisfactorily reproduce the diffraction pattern. The ab initio computational code Dmol was used in determining the torsional barrier associated with phenyl ring rotation. Calculations were performed on a small molecular analogue of the MePBI repeat unit. Full geometry optimization was performed, holding fixed the torsional angle at various positions. The Becke−Perdew−Wang functional, in addition to a double-numeric basis set with polarization functions, were used in all cases. For the calculated X-ray patterns, the crystallite size and degree of misorientation was chosen to best reproduce the experimental pattern. An isotropic temperature factor of 6.0 Å^2 was used for all simulated patterns.

SAXS was performed using the NanoSTAR system, jointly developed by Brüker AXS, Anton Paar GmbH, and the Erich-Schmid-Institute. Cu Kα radiation was used in all experiments. The reported experimental setup of the NanoSTAR system includes a HR-PHK pinhole SAXS camera, a pair of cross-coupled Göbel mirrors, and a Brüker AXS HI-STAR position sensitive area detector. A sample-to-detector distance of 64.8 cm, with a measurement time of ≈17 h, was used in all experiments.

Details of the tensile,[30] compression,[11,12] and torsional[13] test methods used for this work have been reported previously.

Results and Discussion

Figure 2 shows a TGA of as-spun MePBI and MePBZT. In MePBI, a constant weight loss is noted from 25 to 225 °C, with accelerated weight loss occurring around 225 °C. From previously reported TG/MS work, degradation in MePBZT begins around 425 °C with the loss of the pendant group.[9] The increased weight loss, beginning around 450 °C in MePBI, can be attributed to the cleaving of the pendant group. The weight loss in both systems, up to ≈450 °C, is most likely due to the removal of residual (bound or unbound) solvent or water. On the basis of this assumption, TGA shows a greater affinity for the solvent and/or water in MePBI as compared to MePBZT. Structural changes in PIPD, due to the removal of water from the crystal phase, have been observed in WAXD patterns of as-spun fibers.[5] Complete removal of water from PIPD was noted around

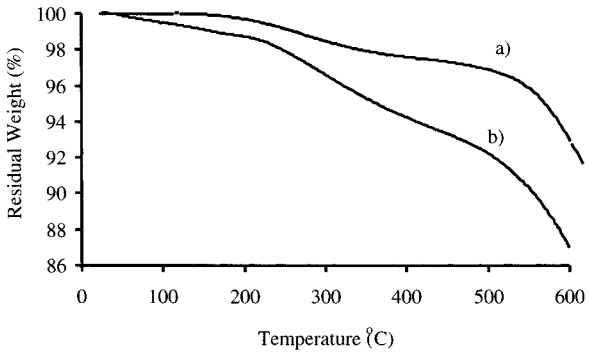

Figure 2. TGA of (a) as-spun MePBZT and (b) as-spun MePBI, vacuum-dried at 100 °C overnight.

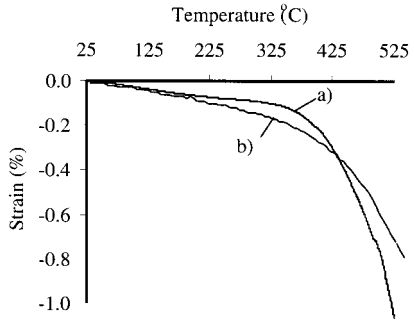

Figure 3. TMA of (a) MePBI and (b) MePBZT fibers tension heat-treated at 390 °C.

330 °C.[14] A progression from the removal of weakly bound water to the removal of more tightly bound water may be the origin of the change in thermogravimetric behavior observed around 225 °C in MePBI. This is partially substantiated from variable temperature FTIR, presented subsequently.

The thermomechanical response of tension heat-treated (at 390 °C) MePBI and MePBZT fibers is given in Figure 3. As is common in rigid-rod polymeric fibers, both MePBI and MePBZT have a negative axial coefficient of thermal expansion (CTE), which remains fairly constant up to about 400 °C (CTE value between −5 and −8 ppm /°C). At about 400 °C the contraction rate increases with temperature in both systems. This accelerated shrinkage is believed to be a result of the onset of cross-linking or other chemical changes occurring with pendant loss. The effects of cross-linking in MePBZT[15] and associated structural changes during pendant loss and /or degradation processes in rigid-rod polymers have been discussed elsewhere.[16]

Hydrogen bonding as a function of temperature has been monitored in aliphatic amorphous[17] and aromatic (PPTA)[18] polyamides using FTIR. In the case of aliphatic polyamides, a systematic shift to higher frequency and decrease in intensity of the N−H absorption band with temperature was attributed to a decrease in the average strength of the hydrogen bond. These spectral changes

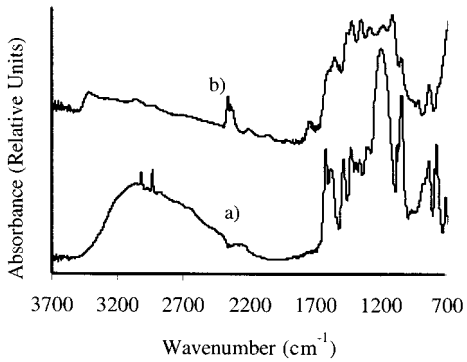

Figure 4. Infrared spectrum of MePBI film at room temperature. Samples have been heat-treated at (a) 350 °C and (b) 500 °C in N_2.

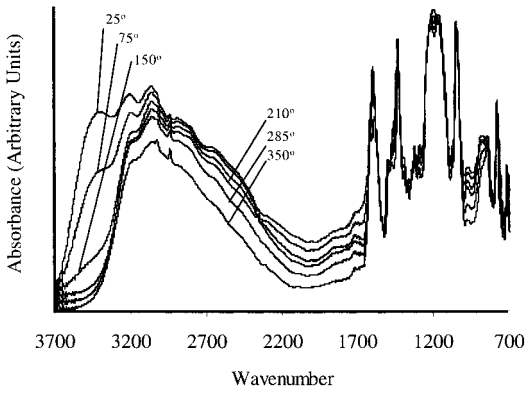

Figure 5. Infrared spectra of MePBI film under N_2 as a function of temperature.

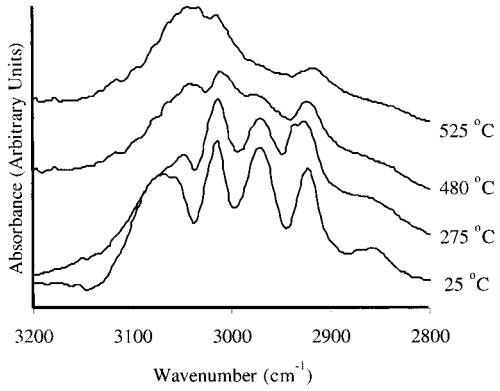

Figure 6. FTIR spectra of MePBZT film at various temperatures under N_2.

were not so apparent in PPTA, with peak position and to some extent absorption, remaining fairly constant up to temperatures as high as 300 °C.[18] In as much as the frequency of the N−H stretching mode is dictated primarily by distance and geometry,[17] conformational rigidity would appear to manifest itself in increased thermal stability of the hydrogen bond in PPTA.

Previously, a set of strong, broad, and complex absorption bands, spanning from ≈2500 to 3300 cm^{-1}, has been reported and assigned to intramolecular hydrogen bonding in hydroxy-PBZT.[7] A similar feature is notable in the IR spectrum of MePBI, given in Figure 4. This broad absorption band is absent in the IR of heat-treated MePBZT[19] because MePBZT does not have strongly associating groups. The broad absorption in MePBI, between 2200 and 3400 cm^{-1}, is assigned to intermolecular hydrogen bonding between N−H and N groups, in addition to any water present within the system. The extreme breadth of this peak can be attributed to the wide distribution of hydrogen bond strengths in the unoriented MePBI film. Other features in the MePBI FTIR spectrum include the sharp aromatic and aliphatic C−H stretching peaks around 3000 cm^{-1}. The stretching modes of conjugated carbon−carbon and carbon−nitrogen double bonds can be located in the region of 1600−1420 cm^{-1}. The sharp peak at 1044 cm^{-1} can be attributed to a C−H in-plane bending mode, while the peaks below 800 cm^{-1} can be assigned to various out-of-plane bending modes. The $C-N_{protonated}$ stretch, located at 1191 cm^{-1}, is revealing in that it shows significant broadening as compared to neighboring peaks. It is well-known that the C−OH stretching band is broadened due to hydrogen bonding in alcohols. Thus, the increased breadth of the $C-N_{protonated}$ band, as compared to others in the fingerprint region, would suggest the amine nitrogen is involved in hydrogen bonding.

The FTIR spectrum of MePBI film after heating to 500 °C under N_2 is also present in Figure 4. As can be seen, the chemical structure of MePBI changes upon heating to temperatures where pendant loss occurs. Most notable is the disappearance of the broad hydrogen bond peak between 2200 and 3300 cm^{-1} as well as the disappearance of the $C-N_{protonated}$ stretching band. The formation of a new peak around 3417 cm^{-1} could be due to the presence of "free" (i.e., not hydrogen-bonded) N−H groups that develop upon the degradation of MePBI.

Figure 5 presents the IR spectra of MePBI film as it undergoes a first heating from room temperature under N_2. An additional peak (as compared to Figure 4), located around 3380 cm^{-1}, is present in the room temperature spectrum, which is attributed to weakly associated water within the system. This peak disappears completely upon heating the sample to 210 °C, which is approximately the temperature at which a transition occurs in the TGA (Figure 2). An expanded view of the C−H stretching region of MePBZT is given in Figure 6. The broad peak around 3075 cm^{-1} may be partially attributed to water, as heating to relatively low temperatures causes much of this peak to disappear. Further heating of MePBZT causes the disappearance of much of the aliphatic C−H stretching bands, which would be attributed to the removal of the methyl-pendant group. Similar reactions would be probable in MePBI. Some residual aliphatic C−H stretching bands may be present in MePBI and MePBZT as uncleaved pendant groups or as methylene cross-links after degradation.[19] Heating MePBI serves to decrease the intensity of the broad hydrogen bonding between 2200 and 3300 cm^{-1}. The reversal of this phenomenon upon cooling from 400 °C is shown in Figure 7, where the primary spectral change as the temperature decreases is an increase in the intensity of the broad peak between 2200 and 3300 cm^{-1}. This increase in absorption intensity can be attributed to an increase in the absorption coefficient through increasing the strength of hydrogen bonding within the system.[17]

The dynamic mechanical responses of tension heat-treated MePBI and MePBZT are given in Figure 8. In MePBI, two transitions, one at 96 °C and one at 360 °C, are apparent, with a shoulder present around 230 °C. These transitions correspond to a decrease in storage modulus to 96, 84, and 53% of the room temperature value. The behavior of MePBZT is somewhat different in that two broad loss processes can be distinguished,

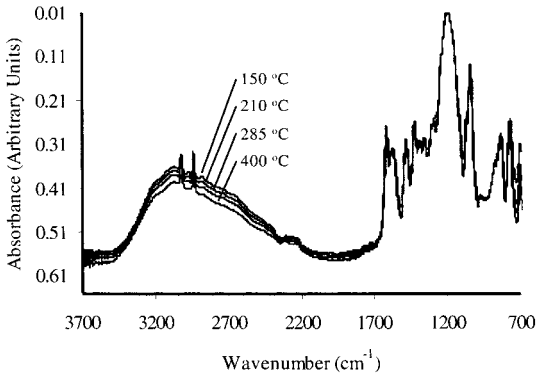

Figure 7. IR spectra of MePBI film during cooling under N_2.

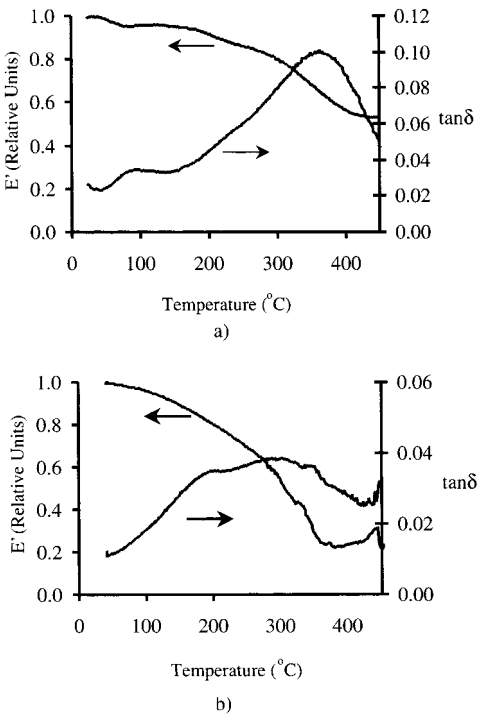

Figure 8. Dynamic mechanical response of (a) MePBI and (b) MePBZT fibers tension heat-treated at 390 °C.

one around 200 °C and the other at 300 °C. As compared to MePBI, MePBZT shows a greater degree of "softening" upon heating, with the storage modulus decreasing to roughly 20% of the room temperature value at 375 °C. The greater tendency for MePBZT to soften upon heating may be related to the lack of strong, intermolecular association. The transitions in MePBI may be correlated to those observed in the TGA (Figure 2). Specifically, at 96 °C the removal of free water begins, around 230 °C the removal of bound water begins, and finally around 400 °C the onset of pendant loss occurs. The latter transition would also be expected to occur in MePBZT if related to pendant loss. However, this is not observed. The onset of molecular motions at comparable temperatures has been reported in other rigid-rod polymers.[20,21] Softening in both systems is abated at around 400 °C. At this temperature, intermolecular cross-linking is expected to take place, which may also explain the slight increase in modulus observed in MePBZT above 400 °C.

A monoclinic unit cell is proposed for the MePBI crystal. The unit cell parameters are given in Table 1, and the crystal structure is given in Figure 9. While discrepancies are noted, this model was found to best

Table 1. Predicted Unit Cell Parameters and Density of MePBI

a (Å)	10.1
b (Å)	4.03
c (Å)	12.09
γ (deg)	80
ρ (g/cm^3)	1.688
Z	2

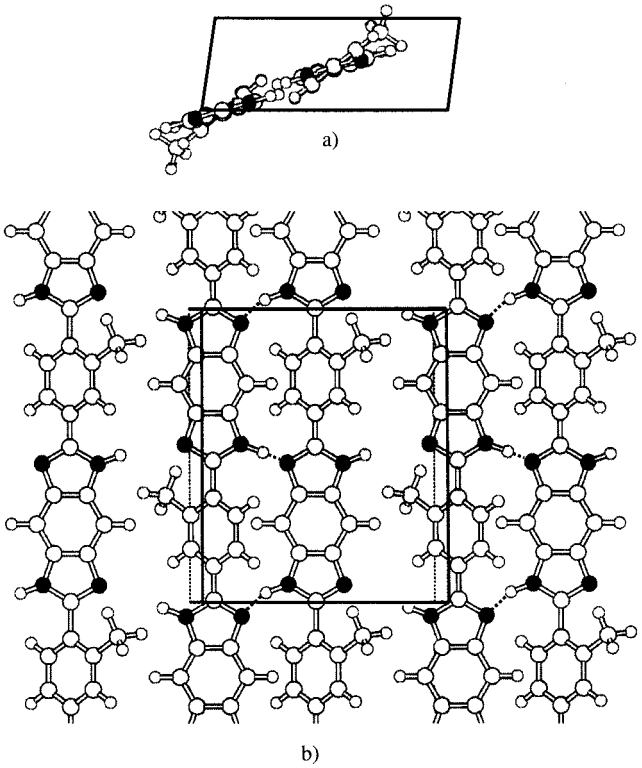

Figure 9. (a) $a-b$ plane and (b) $a-c$ plane of proposed monoclinic crystal structure of MePBI.

reproduce both the meridional and equatorial WAXD patterns, presented in Figure 10. Initially, a hexagonal model, containing two repeat units residing at (0,0,0) and ($^1/_2$,$^1/_2$,0) within the cell, was used to index the equatorial and meridional WAXD patterns. However, a feature that set MePBI apart from other rigid-rod polymers[3,22] was the overwhelming intensity of the (002) reflection at 15.05° 2θ. This could only be accounted for by axially translating one chain in the unit cell by $\approx c/2$. Given this translation, hydrogen bonding could be maximized by rotating the translated repeat unit by 180° about the chain axis, bringing the amine hydrogen and adjacent nitrogen into registry. Another key feature, which differentiated the crystal structure of MePBI from other rigid-rod polymers,[3,23] was the relatively strong equatorial diffraction peak at 8.7° 2θ. The equatorial peaks at 8.7°, 17.6°, and 24.9° were assigned to the (100), (200), and (110) diffraction planes. To produce significant diffraction from the (100) plane, a slight off-centering along the a-axis of the chain located at ($^1/_2$,$^1/_2$,$^1/_2$) was necessary. It was reasoned that the requisite off-centering would only take place if interactions between the repeat unit and its immediate neighbors (i.e., those located at $a - {}^1/_2$ and $a + {}^1/_2$ relative to the repeat unit) were asymmetrical. The necessary asymmetry in interactions could be achieved by "grouping" the methyl-pendant groups, such that pendants on adjacent molecules were directed toward one another. Incentive for this ordering may be brought about through more efficient hydrogen bonding on one "side"

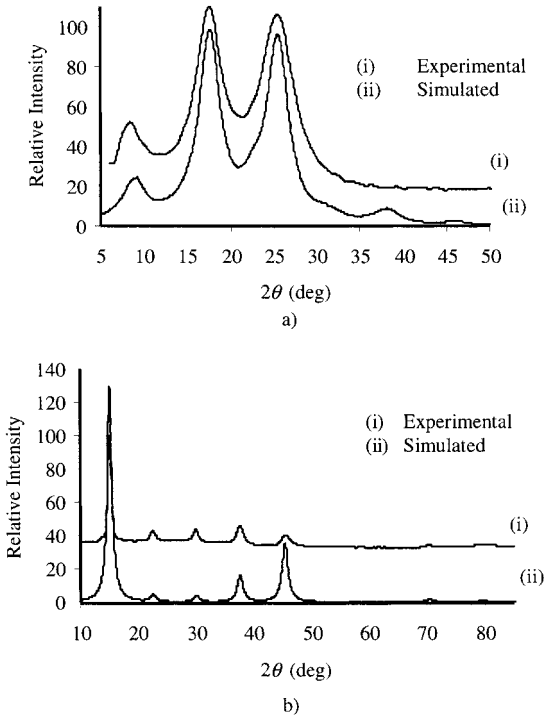

Figure 10. Experimental and simulated WAXD patterns of tension heat-treated MePBI fiber: (a) equatorial and (b) meridional.

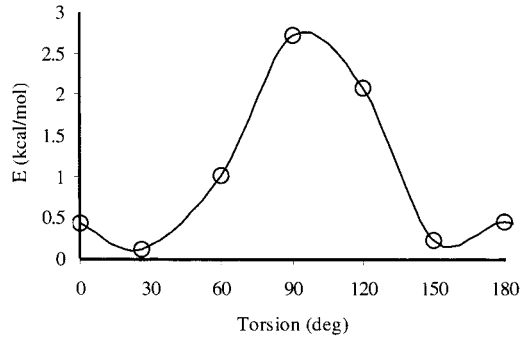

Figure 11. Phenyl ring barrier to rotation in MePBI obtained from DFT.

of the molecule, at the expense of the interactions on the other side (See Figure 9).

A value for the angle, γ, was chosen by taking into account energy considerations, as predicted using atomistic simulation techniques, in addition to fitting the experimental pattern. The torsional angle between the phenyl ring and heterocycle was chosen on the basis of ab initio calculations used to calculate the barrier to rotation. The resulting potential, presented in Figure 11, predicted the energy minimum to be located around 30°. However, given the height of the energy barrier (i.e., the apparent flexibility of this torsion), the torsional angle may take on a different value within the bulk crystalline structure.[24] By immersion of the fiber in various liquids having densities between 1.594 and 1.689 g/cm^3, the density of tension heat-treated MePBI fibers was estimated to be 1.63 g/cm^3, while the calculated density based on the proposed crystal structure is 1.688 g/cm^3.

The proposed MePBI crystal structure allows for the presence of intermolecular hydrogen bonding. However, unlike PIPD, hydrogen bonding is not bidirectional in nature. Rather, it appears that hydrogen bonding occurs between pairs of chains, as the presence of methyl groups prevents its formation on the other side of the chain (see Figure 9). The presence of hydrogen bonding, or lack thereof, is based on comparing N...H−N distances found in MePBI to those found in purines, pyrimidines, nucleosides, and nucleotides. Specifically, in these materials, hydrogen bond distances range from 1.72 to 2.23 Å.[25] In MePBI, where the pendant groups do not provide steric hindrance to packing, the resulting N...H−N distance is measured to be ≈2 Å, whereas the presence of the pendants serves to increase this distance to ≈3 Å. The associated N...H−N angles were found to remain around 170°.

Table 2. Typical Room Temperature Mechanical Properties of Various Rigid-rod Polymeric Fibers

	σ_T (GPa)	E_T (GPa)	ϵ %	σ_c (GPa)[a]	σ_c^{loop} (GPa)[b]	G (GPa)
PBO[c]	5.8	280	2.5	0.34	0.43	1.0
Kevlar 149 (i.e., PPTA)[c]	3.4	185	3	0.36	0.51−0.79	1.1
PIPD[d]	4.0	330	1.2	1.0	1.7	∼3
as−spun MePBZT[e]	1.0	67	2.6	0.59		1.0
HT MePBZT[e]	2.0	128	1.5	0.33	0.46	1.2
as−spun MePBI[e]	1.7	100	2.5	∼0.7		1.3
HT MePBI[e]	2.4	130	1.9	0.71	0.73	3.0

[a] Compressive strength obtained from the recoil compressive stress method, unless otherwise noted. [b] Compressive strength values obtained from the loop test. [c] Values taken from Toyobo technical data on Zylon, refs 26 and 13. [d] Tensile properties have been taken from ref 2. σ_c^{loop} and G have been taken from refs 5 and 14, respectively. σ_c has been taken from refs 2b and 39, measured via the composite and Raman spectroscopy method. [e] Values measured in the present work.

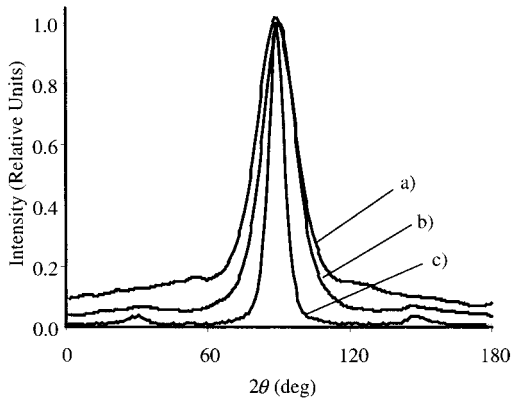

Figure 12. Azimuthal scans of the equatorial peak at ∼25° 2θ of tension heat-treated (a) MePBI, (b) MePBZT, and (c) PBZT fibers tested in this work.

Typical room temperature mechanical properties of various high-performance polymeric fibers, including those for as-spun and tension heat-treated MePBI and MePBZT fibers, are given in Table 2. Tension heat treatment significantly increases the tensile strength and modulus of both MePBI and MePBZT. However, because of poor orientation, the tensile moduli of tension heat-treated MePBI and MePBZT were still comparatively lower than those in other rigid-rod polymers. This is substantiated by comparing azimuthal scans of the tension heat-treated PBZT, MePBZT, and MePBI fibers, presented in Figure 12. The full width at half-maximum, (fwhm) values for these fibers are 8°, 18°, and 22° respectively. It should be noted that the fwhm of tension heat-treated PIPD fiber has been reported to be 10°. Thus, improvements in the tensile moduli of MePBI and MePBZT would be possible with increased orientation. The flat-plate X-ray diffraction pattern of heat-treated

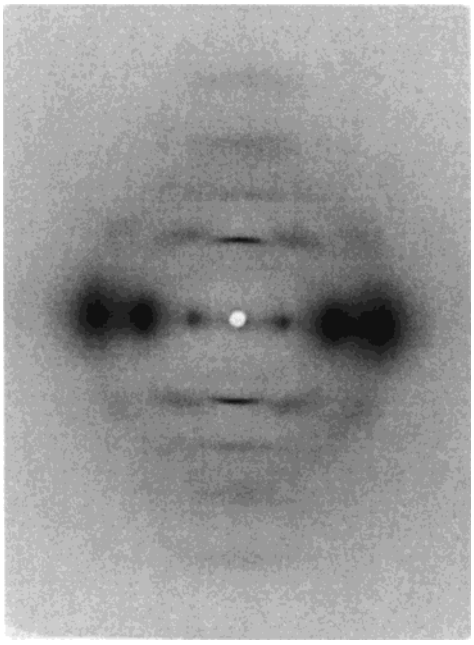

Figure 13. Experimental flat-plate WAXD patterns of tension heat-treated MePBI.

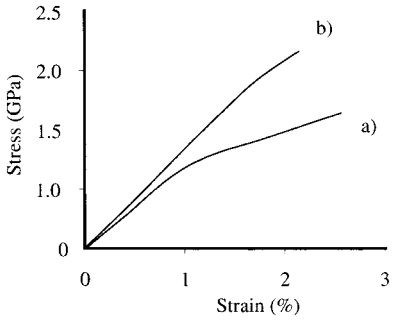

Figure 14. Typical stress vs strain curves of (a) as-spun and (b) tension heat-treated MePBI fiber.

MePBI fiber shown in Figure 13, exhibits lack of three-dimensional order in the sample.

Similar to previous observations,[30] as-spun fibers of both MePBI and MePBZT were found to have abnormally high recoil compressive strength values. Most likely, this is due to energy losses occurring in the fiber during testing.[30] Examples of yielding in as-spun and heat-treated MePBI fibers are shown in the stress versus strain curves in Figure 14. Tension heat-treated MePBI fiber behaves in a more brittle-like manner, but still shows nonlinearly in the stress−strain curve, most likely because of poor molecular orientation. The recoil compressive strength of tension heat-treated MePBI was measured to be 0.71 GPa. This comparatively high recoil compressive strength value can be attributed to improved intermolecular interactions via hydrogen bonding. Conversely, the recoil compressive strength of tension heat-treated MePBZT decreased to 0.33 GPa, which is comparable to the value previously reported for MePBZT,[13] as well as those measured on other rigid-rod systems where only van der Waals interactions are present.[26] The influence of strong intermolecular interactions can also be seen in the higher torsional modulus of MePBI over MePBZT. The torsional modulus of heat-treated MePBI is comparable to that of PIPD (Table 2). Compressive strength of heat-treated MePBI and MePBZT, as measured by the elastica loop test, are also given in Table 2. It should be noted, however, that for these fibers it is not known if the compressive and tensile moduli are equivalent; an assumption that was made in calculating the compressive strength from the elastica loop test. These factors notwithstanding, the compressive strength of MePBI fiber is higher than that of PBO and PBZT fibers. By comparison, the PIPD fiber heat-treated at 200 °C is reported to have a loop compressive strength of 1.7 GPa,[5] which upon heat treatment to 400 °C, decreased to 1.1 GPa.[5] However, the appearance of longitudinal cracks in fibers heat-treated at 400 °C was reportedly at fault in lowering the PIPD compressive strength.[5] On the basis of the low tensile modulus measured for the MePBI fibers, further improvement in compressive strength may be expected by producing higher orientation, which would enhance order and maximize intermolecular association via hydrogen bonding.

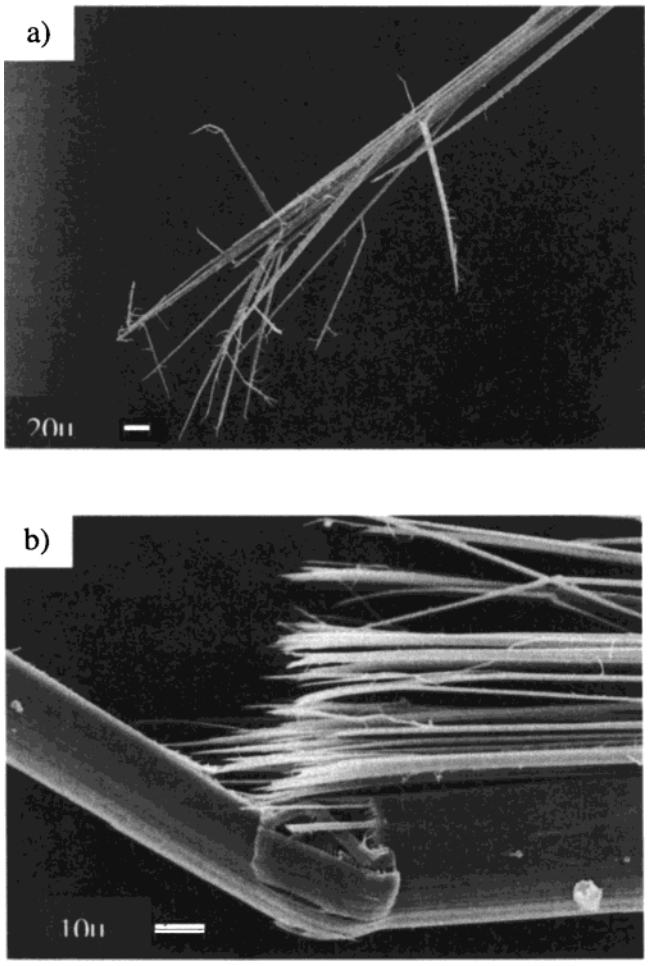

Figure 15. Scanning electron micrographs of (a) tensile and (b) compressive failure in MePBI fiber tension heat-treated at 390 °C.

Compressive failure has been thought to be governed by fibrillar rather than molecular instability.[27,28] It was of some interest, therefore, to examine the morphology of MePBI. Figure 15 shows tensile and compressive failure in MePBI fiber. Tension heat-treated MePBI fiber shows a highly fibrillar morphology, common to rigid-rod polymers.[29,30] Longitudinal cracks, presumably due to interfibrillar rupture, are evident in Figure 15b. Likewise, these features are also not unique to MePBI.[31−33]

SAXS patterns of MePBZT and MePBI fibers are presented in Figure 16. Apparent in both fibers is the

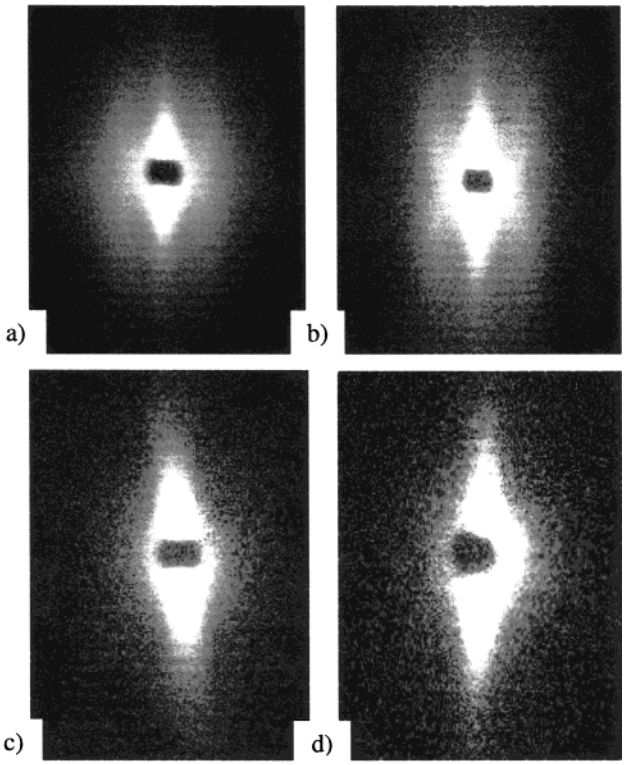

Figure 16. SAXS of (a) MePBZT fiber tension heat-treated at 390 °C for 5 min, (b) MePBZT fiber tension heat-treated at 390 °C for 5 min and subsequently free-annealed at 490 °C for 10 min, (c) MePBI fiber tension heat-treated at 425 °C for 2 min, and (d) MePBI fiber tension heat-treated at 425 °C for 2 min and subsequently free-annealed at 490 °C for 10 min. *The fiber axis is orientated horizontally.*

typical equatorial streaking, which is generally attributed to the presence of elongated voids[34] or crystals.[35] Moreover, a four-point SAXS pattern is observed in MePBZT, suggesting regions of electron density variations in the axial direction. This pattern is not unlike that observed in various rigid-rod polymeric systems and has been enumerated elsewhere.[36] The SAXS of heat-treated MePBI fibers show a lack of a well-developed four-point pattern.

Now the question is what accounts for high compressive strength in MePBI? Is it hydrogen bonding? On the basis of the proposed MePBI crystal structure, which only shows hydrogen bonding between two adjacent PBI chains in transverse directions, it appears that hydrogen bonding may not be responsible for high compressive strength in MePBI. However, it is envisioned that crystalline defects may exist within the structure, which may allow for the association of more than two polymer chains. In particular, a defect where a repeat unit in a given polymer chain is rotated 180° with respect to its predecessor, would make it possible to form hydrogen bonds between several adjacent chains. Such a defect is thought to occur in PBO.[37] The presence of the methyl-pendant group in MePBI would seemingly make this defect more costly in terms of energy; however, if repeated sparsely along a chain, this defect would allow for the formation of a sheetlike hydrogen-bonded structure. The envisioned repeat unit rotation and resulting hydrogen-bonded structure is illustrated in Figure 17.

The aromatic polyamide, PPTA, forms a sheetlike arrangement of hydrogen bonds and has a recoil compressive strength of 0.36 GPa. Thus, other factors in addition to hydrogen bonding may be responsible for the

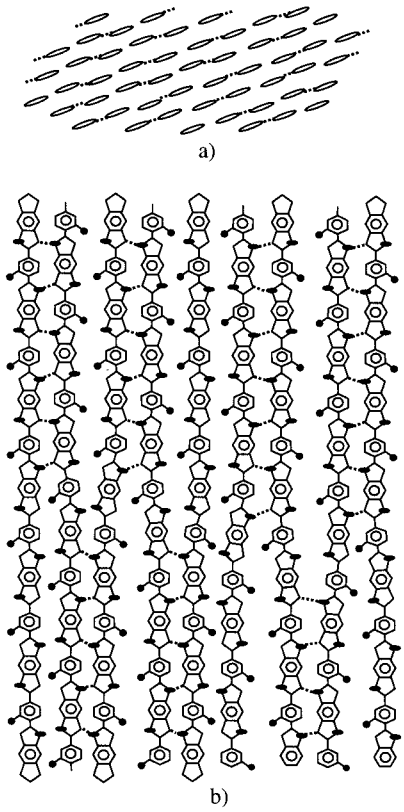

Figure 17. Schematic representation of hydrogen bonding in MePBI: (a) $a-b$ plane and (b) $a-c$ plane.

relatively high compressive strength of MePBI. More specifically, chain flexibility (i.e., conformational flexibility) may also influence the compressive strength of these materials. The compressive strength of the aromatic polyamide, PPTA, is twice the compressive strength of the aromatic copolyester poly(*p*-hydroxy benzoic acid-*co*-naphthoic acid) (i.e., Vectran, $\sigma_c^{recoil} = 0.18$ GPa).[38] Neglecting any morphological differences, the formation of hydrogen bonds in PPTA would seem to play a fairly substantial role in accounting for the compressive strength difference between Kevlar and Vectran, as both have some conformational flexibility; however, there is no hydrogen bonding in Vectran. In a comparison of Vectran and the rigid-rod polymer PBZT, two systems that both form weak intermolecular interactions, PBZT has a somewhat higher recoil compressive strength (0.3 GPa). Again, neglecting morphology differences, one may conclude that the comparatively rigid structure of PBZT contributes to its higher compressive strength, as compared to that of Vectran. However, it must be kept in mind that morphological differences and other defects may also influence compressive strength.

The difference in the recoil compressive strengths of PBZT and MePBI may be due to hydrogen bonding. Thus, both conformational flexibility as well as intermolecular interactions may play a role in determining the compressive strength. The relatively high compressive strength of PIPD over MePBI may be due to the difference in dimensionality of the hydrogen bond network (i.e., bidirectional vs planar). However, as mentioned above, an improvement in molecular orientation could improve the hydrogen bonding in MePBI, which would further increase its compressive strength. Summarizing, the bidirectional nature of the hydrogen-bonded network in PIPD would seem to account for only a part of the increase in the compressive strength over

Table 3. Coordinate File for an MePBI Crystal Cell

	chain 1				chain 2		
	x	*y*	*z*		*x*	*y*	*z*
C1	0.0065	0.0404	−0.0082	C16	0.5838	0.5207	0.4693
C2	0.1222	0.1073	0.4622	C17	0.4706	0.4302	0.5263
C3	−0.1069	−0.0578	0.0475	C18	0.3802	0.3524	0.4975
C4	−0.0603	−0.0264	0.1546	C19	0.5150	0.4753	0.6327
C5	−0.1289	−0.0889	0.2544	C20	0.4458	0.4253	0.7327
C6	−0.2310	−0.1726	0.2541	C21	0.3437	0.3409	0.7330
C7	−0.0597	−0.0384	0.3544	C22	0.5142	0.4891	0.8325
C8	−0.1051	−0.0768	0.4608	C23	0.4682	0.4541	0.9396
C9	−0.1958	−0.1515	0.4897	C24	0.6973	0.6187	0.5249
C10	0.1197	0.1312	0.0488	C25	0.6507	0.5874	0.6320
C11	0.2101	0.2092	0.0200	C26	0.7193	0.6497	0.7318
C12	0.0753	0.0861	0.1553	C27	0.8215	0.7332	0.7316
C13	0.1445	0.1362	0.2553	C28	0.6501	0.5995	0.8319
C14	0.2465	0.2208	0.2556	C29	0.6955	0.6377	0.9383
C15	0.0761	0.0722	0.3551	C30	0.7863	0.7122	0.9671
H1	0.0080	0.0150	0.5179	H11	0.5823	0.5461	0.9953
H10	0.0076	0.0217	0.6451	H12	0.5827	0.5395	1.1226
H2	0.0864	0.2503	0.7019	H13	0.5040	0.3106	1.1793
H3	0.0861	0.2564	0.8177	H14	0.5043	0.3046	1.2951
H4	0.1474	0.4344	0.8618	H15	0.4430	0.1264	1.3393
H5	0.1735	0.4951	0.6370	H16	0.4171	0.0657	1.1144
H6	0.2718	0.3904	0.6270	H17	0.3187	0.1703	1.1044
H7	0.1302	0.5398	0.5558	H18	0.4603	0.0210	1.0333
H8	0.1801	0.7286	0.6821	H19	0.4104	−0.1678	1.1596
H9	−0.0715	−0.2010	0.7042	H20	0.6618	0.7623	1.1816
N1	−0.1329	−0.3790	0.6600	N5	0.7231	0.9405	1.1374
N2	−0.0719	−0.1949	0.8199	N6	0.6622	0.7562	1.2974
N3	−0.1335	−0.3682	0.8659	N7	0.7238	0.9297	1.3434
N4	0.0069	0.0338	0.8767	N8	0.5834	0.5274	1.3541

that of other rigid-rod polymers, as the introduction of planar hydrogen bonding within the system also leads to improvement.

Acknowledgment. SAXS patterns were obtained by Dr. R. Görgl of Anton Paar GmbH/Erich-Schmid-Institut (Leoben, Austria). This effort was partially sponsored by the Air Force Office of Scientific Research, Air Force Materials Command, USAF, under Grant F49620-00-1-0147. The U.S. Government is authorized to reproduce and distribute reprints for Government purposes notwithstanding any copyright notation thereon.

Disclaimer. The views and conclusions contained herein are those of the authors and should not be interpreted as necessarily representing the official policies or endorsements, either expressed or implied, of the Air Force Office of Scientific Research or the U.S. Government.

Appendix

See Table 3.

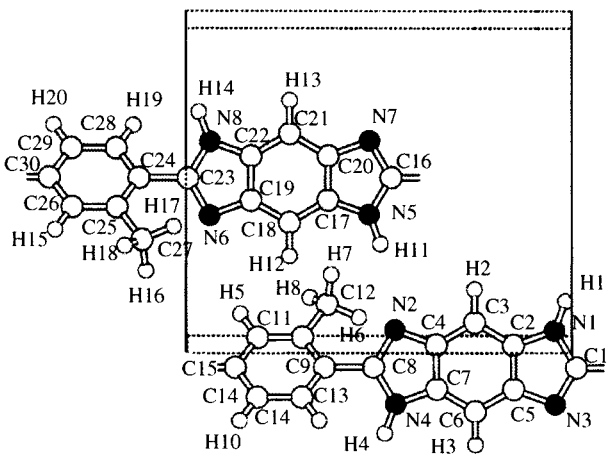

References and Notes

(1) Kumar, S.; Helminiak, T. *SAMPE J*. **1990**, *26*.
(2) (a) Sikkema, D. J. *Polymer* **1998**, *39*, 5981. (b) Sikkema, D. J. *The Fiber Society Book of Abstracts*; Mulhouse: France, 1997.
(3) Klop, E. A.; Lammers, M. *Polymer* **1998**, *39*, 5987.
(4) Hageman, J. C. L.; van der Horst, J. W.; de Groot, R. A. *Polymer* **1999**, *40*, 1313.
(5) Lammers, M.; Klop, E. A.; Northolt, M. G.; Sikkema, D. J. *Polymer* **1998**, *39*, 5999.
(6) Arnold, F. E. *Mater. Res. Soc. Symp. Proc.* **1989**, *134*, 75.
(7) Tan, L.-S.; Arnold, F. E.; Dang, T. D.; Chuah, H. H.; Wei, K. H. *Polymer* **1994**, *35*, 3091.
(8) So, Y.-H. *Prog. Polym. Sci.* **2000**, *25*, 137.
(9) Dang, T. D.; Wang, C. S.; Click, W. E.; Chuah, H. H.; Tsai, T. T.; Husband, D. M.; Arnold, F. E. *Polymer* **1997**, *38*, 621.
(10) Dang, T. D.; Arnold, F. E., unpublished results.
(11) Allen, S. R. *J. Mater. Sci.* **1987**, *22*, 853.
(12) Sinclair, D. *J. Appl. Phys.* **1950**, *21*, 380.
(13) Mehta, V. R.; Kumar, S. *J. Mater. Sci.* **1994**, *29*, 3658.
(14) Lammers, M. Ph.D. Thesis, Swiss Federal Institute of Technology, Zurich, 1998.
(15) Jenkins, S.; Jacob, K. I.; Kumar, S. *J. Polym. Sci.: Polym. Phys.* **1998**, *36*, 3057.
(16) Jenkins, S.; Jacob, K. I.; Polk, M. B.; Kumar, S.; Dang, T. D.; Arnold, F. E., in preparation.
(17) Skrovanek, D. J.; Howe, S. E.; Painter, P. C.; Coleman, M. M. *Macromolecules* **1985**, *18*, 1676.
(18) Siesler, H. W.; Holland-Moritz, K. *Infrared and Raman Spectroscopy of Polymers*; Marcel Dekker: New York, 1980; Vol. 4.
(19) Mehta, V. R.; Kumar, S.; Polk, M. B.; VanderHart, D. L.; Arnold, F. E.; Dang, T. D. *J. Polym. Sci.: Polym. Phys.* **1996**, *34*, 1881.
(20) Mactuck, K. S.; Eby, R. K.; Farmer, B. L. *Polymer* **1994**, *35*, 53.
(21) Kuroki, T.; Tanaka, Y.; Hokudoh, T.; Yabuki, K. *J. Appl. Polym. Sci*. **1997**, *65*, 1031.
(22) Lenhert, P. G.; Adams, W. W. *Mater. Res. Soc. Symp. Proc.* **1989**, *134*, 329.
(23) Fratini, A. V.; Lenhert, P. G.; Resch, T. J.; Adams, W. W. *Mater. Res. Soc. Symp. Proc.* **1989**, *134*, 431.
(24) Trohalaki, Dudis, D. S. *Polymer* **1995**, *36*, 991.
(25) Jeffrey, G. A. *An Introduction to Hydrogen Bonding*; Oxford University Press: New York, 1997; p 66.
(26) Kozey, V. V.; Jiang, H.; Mehta, V. R.; Kumar, S. *J. Mater. Res.* **1995**, *10*, 1044.
(27) C. Lee, Y.-C.; Santhosh, U. *Polym. Eng. Sci*. **1993**, *33*, 907.
(28) Rein, D. M.; Cohen, Y. *J. Mater. Sci*. **1995**, *30*, 3587.
(29) Martin, D. C.; Thomas, E. L. *Mater. Res. Soc. Symp. Proc.* **1989**, *134*, 415.
(30) Mehta, V. R.; Kumar, S. *J. Appl. Polym. Sci*. **1999**, *73*, 305.
(31) Dobb, M. G.; Johnson, D. J.; Savill, B. P. *Polymer* **1981**, *22*, 960.
(32) Martin, D. C.; Thomas, E. L. *Mater. Res. Soc. Symp. Proc.* **1989**, *134*, 465.
(33) Sahafeyan, M.; Kumar, S. *J. Appl. Polym. Sci*. **1995**, *56*, 517.
(34) Minter, J. R.; Ph.D. Thesis, University of Massachusetts, 1982.
(35) Grubb, D. T.; Prasad, K.; Adams, W. W. *Polymer* **1991**, *32*, 1167.
(36) Kumar, S.; Warner, S.; Grubb, D. T.; Adams, W. W. *Polymer* **1994**, *35*, 5408.
(37) Tashiro, K.; Yoshino, J.; Kitagawa, T.; Murase, H.; Yabuki, K. *Macromolecules* **1998**, *31*, 5430.
(38) Bai, Y. M.S. Thesis, Georgia Institute of Technology, 1998.
(39) Sirichaisit, J.; Young, R. J. *Polymer* **1999**, *40*, 3421.

MA000790X